

EXTRAGALACTIC BACKGROUND LIGHT FROM HIERARCHICAL GALAXY FORMATION: GAMMA-RAY ATTENUATION UP TO THE EPOCH OF COSMIC REIONIZATION AND THE FIRST STARS

YOSHIYUKI INOUE¹, SUSUMU INOUE^{2,3}, MASAKAZU A. R. KOBAYASHI⁴, RYU MAKIYA⁵, YUU NIINO⁶, & TOMONORI TOTANI⁵

¹Kavli Institute for Particle Astrophysics and Cosmology, Department of Physics, Stanford University and SLAC National Accelerator Laboratory, 2575 Sand Hill Road, Menlo Park, CA 94025, USA

²Max-Planck-Institut für Kernphysik, Saupfercheckweg 1, 69117 Heidelberg, Germany

³Institute for Cosmic Ray Research, University of Tokyo, Kashiwa, Chiba 277-8582, Japan

⁴Research Center for Space and Cosmic Evolution, Ehime University, Bunkyo-cho, Matsuyama 790-8577, Japan

⁵Department of Astronomy, Kyoto University, Sakyo-ku, Kyoto 606-8502, Japan and

⁶Optical and Infrared Astronomy Division, National Astronomical Observatory of Japan, Mitaka, Tokyo 181-8588, Japan

Draft version December 10, 2012

ABSTRACT

We present a new, publicly available model of the extragalactic background light (EBL) and corresponding $\gamma\gamma$ opacity for intergalactic gamma-ray absorption from $z = 0$ up to $z = 10$, based on a semi-analytical model of hierarchical galaxy formation that reproduces key observed properties of galaxies at various redshifts. Including the potential contribution from Population III stars in a simplified way, the model is also broadly consistent with available data concerning cosmic reionization, particularly the Thomson scattering optical depth constraints from *WMAP*. In comparison with previous EBL studies up to $z \sim 3$ –5, our predicted $\gamma\gamma$ opacity is in general agreement for observed gamma-ray energy below $400/(1+z)$ GeV, whereas it is a factor of ~ 2 lower above this energy because of a correspondingly lower cosmic star formation rate, even though the observed UV luminosity is well reproduced by virtue of our improved treatment of dust obscuration and direct estimation of star formation rate. The horizon energy at which the gamma-ray opacity is unity does not evolve strongly beyond $z \sim 4$ and approaches ~ 20 GeV. The contribution of Population III stars is a minor fraction of the EBL at $z = 0$, and is also difficult to distinguish through gamma-ray absorption in high- z objects, even at the highest levels allowed by the *WMAP* constraints. Nevertheless, the attenuation due to Population II stars should be observable in high- z gamma-ray sources by telescopes such as *Fermi* or CTA and provide a valuable probe of the evolving EBL in the rest-frame UV.

Subject headings: cosmology: diffuse radiation – gamma rays : theory

1. INTRODUCTION

The extragalactic background light (EBL), the diffuse, isotropic background radiation from far-infrared (FIR) to ultraviolet (UV) wavelengths, is believed to be predominantly composed of the light from stars and dust integrated over the entire history of the Universe (see Dwek & Krennrich 2012, for reviews). The observed spectrum of the local EBL at $z = 0$ has two peaks of comparable energy density. The first peak in the optical to the near-infrared (NIR) is attributed to direct starlight, while the second peak in the FIR is attributed to emission from dust that absorbs and reprocesses the starlight.

The precise determination of the EBL has been a difficult task. Direct measurements of the EBL in the optical and NIR bands have been hampered by bright foreground emission caused by interplanetary dust, the so-called zodiacal light (see Hauser & Dwek 2001, for reviews). Recently, Matsuoka et al. (2011) reported measurements of the EBL at $0.44 \mu\text{m}$ and $0.65 \mu\text{m}$ from outside the zodiacal region using observational data from *Pioneer 10/11*. On the other hand, integration over galaxy number counts provide a firm lower bound on the EBL, and the observed trend of the counts with magnitude indicates that the EBL at $z = 0$ has been largely resolved into discrete sources in the optical/NIR bands (e.g. Madau & Pozzetti 2000; Totani et al. 2001; Keenan et al. 2010), even when the effect of incomplete detection due to cosmological dimming of surface brightness is taken into account (Totani et al. 2001).

The EBL can also be probed indirectly through observa-

tions of high-energy gamma rays from extragalactic objects (e.g. Mazin & Raue 2007). Gamma-rays propagating through intergalactic space can be attenuated by photon-photon pair production interactions ($\gamma\gamma \rightarrow e^+e^-$) with low-energy photons of the EBL. For gamma-rays of given energy E_γ , the pair production cross section peaks for low-energy photons with energy

$$\epsilon_{\text{peak}} \simeq \frac{2m_e^2 c^4}{E_\gamma} \simeq 0.5 \left(\frac{1 \text{ TeV}}{E_\gamma} \right) \text{ eV}, \quad (1)$$

where m_e is the electron mass and c is the speed of light. In terms of wavelength, $\lambda_{\text{peak}} = 1.24(E_\gamma[\text{TeV}])\mu\text{m}$. Measuring the resultant attenuation features in the spectra of extragalactic GeV-TeV sources would offer a valuable probe of the EBL that is indirect, yet unique in being redshift-dependent. Although this method can be limited by incomplete knowledge of the intrinsic spectra of the source before attenuation, by assuming a plausible range for such spectra, observations of blazars by current ground-based telescopes have been able to place relatively robust upper limits to the EBL at $z = 0$ and up to $z \sim 0.5$ (e.g. Aharonian et al. 2006a; Albert et al. 2008). Combined with the lower limits from galaxy counts, the total EBL intensity at $z = 0$ from $0.1 \mu\text{m}$ to $1000 \mu\text{m}$ is inferred to lie in the range 52 – $99 \text{ nW/m}^2/\text{sr}$ (Horiuchi et al. 2009). However, the EBL at higher redshifts is still highly uncertain.

Currently available theoretical models for the EBL can be broadly categorized into three types. First, in backward evolution models, one starts from the observed properties of galaxies in the local Universe and describes their evolution

by extrapolating backwards in time in a parameterized fashion (e.g. Malkan & Stecker 1998; Totani & Takeuchi 2002; Stecker et al. 2006; Franceschini et al. 2008). This extrapolation entails uncertainties in the properties of the EBL that inevitably increase at high redshifts. Nevertheless, based on the observed, rest-frame K-band luminosity function (LF) of galaxies from $z = 0$ up to $z = 4$, Domínguez et al. (2011) were able to model the EBL without any assumptions for the LF. Helgason & Kashlinsky (2012); Stecker et al. (2012) constructed evolving EBL models in a relatively robust way by utilizing multiwavelength photometric survey data.

Secondly, in forward evolution models, the basis is a description for the cosmic star formation history (CSFH), over which models for the spectral energy distribution (SED) of the stellar population are convolved to obtain the evolving EBL (e.g. Kneiske et al. 2004; Finke et al. 2010). However, such models cannot follow the detailed evolution of key physical quantities such as the metallicity and dust content, which can significantly affect the spectral shape of the EBL. Furthermore, although most forward evolution models employ the CSFH of Hopkins & Beacom (2006), it is known that this CSFH model overproduces the stellar mass density (Choi & Nagamine 2012), and is also inconsistent with the observed rate of core-collapse supernovae (Horiuchi et al. 2011). Recent studies by Kobayashi et al. (2012) show that Hopkins (2004); Hopkins & Beacom (2006) may have overestimated the CSFH at $z > 1$, arising from overcorrection for dust obscuration effects and in conversion from luminosity to star formation rate.

Finally, rooted in the modern cosmological framework of large-scale structure formation driven by cold dark matter, semi-analytical models of hierarchical galaxy formation account for the merging history of dark matter halos as well as the physical evolution of the baryonic component, including the effects of gas cooling, star formation, metal enrichment, feedback heating, etc. (Primack et al. 2005; Gilmore et al. 2009; Younger & Hopkins 2011; Gilmore et al. 2012). Such models successfully reproduce various observed properties of galaxies from the local Universe up to $z \sim 6$ (see e.g., Kauffmann et al. 1993; Cole et al. 1994; Nagashima et al. 1999; Somerville & Primack 1999; Nagashima & Yoshii 2004; Baugh et al. 2005; Nagashima et al. 2005; Kobayashi et al. 2007, 2010; Somerville et al. 2012). At present, semi-analytical models can be considered the most detailed and well-developed models for the EBL over a wide range of redshifts.

A subject that has yet to be fully explored in the context of the EBL and gamma-ray absorption is the epoch of cosmic reionization above $z \sim 6$. Measurements of NIR absorption troughs in the spectra of high- z quasars, together with those of anisotropies in the polarization of the cosmic microwave background (CMB), prove that the majority of intergalactic hydrogen in the Universe has been reionized somewhere between $z \sim 1000$ and $z \sim 6$ (see e.g. Robertson et al. 2010). Although the most widely suspected source of reionization is UV photons emitted by early generations of massive stars, the observational constraints are still very limited, so that the actual sources, history and topology of cosmic reionization remain largely unknown. A closely related topic is the possible existence and formation history of Population III (Pop-III) stars, very massive stars that are expected to originate in nearly metal-free conditions, particularly for the very first generation of stars appearing in the Universe, and their potential role in cosmic reionization (see e.g. Fernandez et al.

2012).

Since the current observational constraints on reionization all concern the neutral or ionized intergalactic gas, it would be very valuable and complementary to obtain independent information on the evolving, UV intergalactic radiation field itself. A unique and promising approach may be offered by the effects of gamma-ray absorption in-situ in high-energy sources at $z > 6$. UV radiation fields with sufficient intensities to cause cosmic reionization may induce significant gamma-ray absorption at observer energies above a few tens of GeV (Oh 2001; Inoue et al. 2010a). Based on a semi-analytical model of galaxy formation that includes Pop-III stars and reproduces a variety of reionization-related observations (Choudhury & Ferrara 2006), the recent study by Inoue et al. (2010a) suggested that appreciable attenuation may be expected above ~ 12 GeV at $z \sim 5$ and down to $\sim 6-8$ GeV at $z \gtrsim 8-10$, mainly caused by Pop-II stars at these epochs. However, the relative contribution of Pop-III stars was found to be difficult to discern observationally. On the other hand, without addressing the implications for reionization, some studies have concentrated on the prospects for constraining Pop-III star formation through gamma-ray absorption in objects at lower redshifts (e.g. Gilmore 2012).

The Fermi gamma-ray space telescope (Atwood et al. 2009, *Fermi*) may eventually detect blazars at $z > 6$ (Inoue et al. 2011), and the Cherenkov Telescope Array (Actis et al. 2011, CTA) may possibly do the same for gamma-ray bursts (GRBs) (Inoue et al. in preparation). Therefore a deeper investigation into the above issues is worthwhile and timely. The above studies (Oh 2001; Inoue et al. 2010a; Gilmore 2012) have not accounted consistently for the EBL resulting from galaxy formation at lower redshifts. For example, the model of Inoue et al. (2010a) was optimized to describe the reionization epoch and did not include the contribution from Pop-I stars or dust, and thus could only evaluate the gamma-ray opacity above $z = 4$.

In this paper, we present a new study of the EBL and consequent gamma-ray opacity, covering the entire redshift range from $z = 0$ up to $z = 10$ within a consistent framework, accounting for the process of cosmic reionization, and including Pop-III stars in a simplified way. As a baseline model, we adopt the Mitaka model¹ of semi-analytical galaxy formation (Nagashima & Yoshii 2004). The model can reproduce various observed properties of galaxies such as the luminosity function (LF), luminosity density (LD), and stellar mass density (Nagashima & Yoshii 2004), as well as the LFs of high-redshift Lyman-break galaxies (LBGs) and Lyman- α emitters (LAEs) up to $z \sim 6$ (Kobayashi et al. 2007, 2010). As regards Pop-III stars, in view of the presently large theoretical uncertainties on their formation efficiency, metal yield, conditions for transition to Pop-II star formation, etc., we choose not to fully incorporate them into our semi-analytical scheme. Instead, their formation history is characterized in a simple, parameterized way, which we constrain by modeling the cosmic reionization process and comparing with available observations, particularly the Thomson scattering optical depth measured by the Wilkinson Microwave Anisotropy Probe (WMAP).

We introduce our semi-analytical model in §2. Cosmic reionization is modeled and compared with observations in §3. §4 presents the results of our EBL models. The con-

¹ Named after the city of Mitaka where the model was mainly developed at the National Astronomical Observatory of Japan.

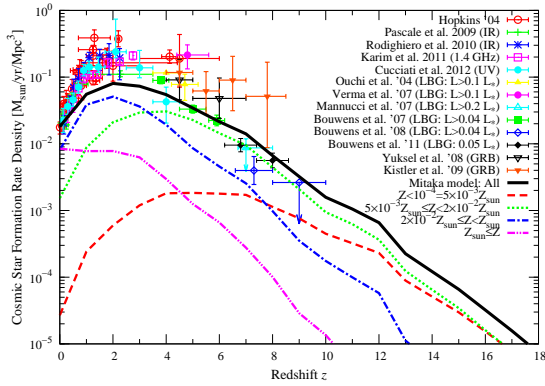


FIG. 1.— Cosmic star formation history. Solid curve shows the total in the baseline Mitaka model, while the dashed, dotted, dot-dashed and double-dot-dashed curves show the fractional contributions from stars with metallicity $Z < 10^{-4} = 5 \times 10^{-3} Z_{\odot}$, $5 \times 10^{-3} Z_{\odot} \leq Z < 2 \times 10^{-2} Z_{\odot}$, $2 \times 10^{-2} Z_{\odot} \leq Z < Z_{\odot}$, and $Z_{\odot} \leq Z$, respectively. We also plot the observational data compiled by Hopkins (2004), that deduced from LBGs (Ouchi et al. 2004; Bouwens et al. 2007; Mannucci et al. 2007; Verma et al. 2007; Bouwens et al. 2008), and that inferred from GRBs (Yüksel et al. 2008; Kistler et al. 2009). For the LBG sample, limiting luminosities adopted by each author are indicated in the corresponding legend in term of the characteristic luminosity L_* of the luminosity function.

sequent gamma-ray opacity and comparison with current gamma-ray observations are described in §5. We conclude in §6. Throughout this paper, we adopt the standard cosmological parameters of $(h, \Omega_M, \Omega_{\Lambda}) = (0.7, 0.3, 0.7)$, and a Salpeter initial mass function (IMF; Salpeter 1955) within a mass range of $0.1 - 60 M_{\odot}$.

2. SEMI-ANALYTICAL GALAXY FORMATION MODEL

In the framework of the Mitaka semi-analytical model of galaxy formation, we compute the evolution of baryon components within dark matter halos following the merger history of dark matter halos. The time evolution of baryons in halos is computed with physically motivated, phenomenological prescriptions for radiative cooling, star formation, supernova feedback, chemical enrichment, and galaxy mergers. Then, we can derive various physical and observational quantities for galaxies as well as the global average over the Universe at any redshift, such as the CSFH, LFs, and dust content of galaxies. A mock catalog of galaxies can be generated, to be compared with various observations. Details of the Mitaka model are described in Nagashima & Yoshii (2004); Kobayashi et al. (2007, 2010).

Since there are several free parameters in the phenomenological prescriptions for baryons, we fix them to fit various observational data of the local galaxies such as B-band and K-band LFs, neutral gas fraction, and gas mass-to-luminosity ratio as a function of B-band luminosity (Nagashima & Yoshii 2004). For consistency, we keep these parameters unchanged in this paper.

2.1. Cosmic Star Formation History

Fig. 1 shows the CSFH expected in the Mitaka model at $z = 0 - 18$. The CSFHs at various metallicity bins are also shown. Pop-III stars are expected to form from gas with metallicity below a critical value, such that the gas can only cool rather inefficiently through rotational transitions of molecular hydrogen, which leads to fragmentation into relatively massive protostellar clouds, and ultimately the formation of very massive stars. Once the metallicity exceeds this

value, the gas can cool more efficiently via metal transitions, and a transition to the formation of less massive, Population II (Pop-II) stars is thought to take place (Mackey et al. 2003; Bromm & Loeb 2003; Yoshida et al. 2004). However, the exact value of this critical metallicity has been hotly debated, ranging from $Z = 10^{-6} Z_{\odot} = 10^{-7.7}$ (Schneider et al. 2006) to $Z = 10^{-2} Z_{\odot} = 10^{-3.7}$ (Aykutalp & Spaans 2011)². In this paper, we consider stars with metallicity $Z < 10^{-4}$ to correspond to Pop-III stars. We adopt a Salpeter IMF in the mass range of $0.1 - 60 M_{\odot}$ for all types of stars. Recent radiation-hydrodynamics simulations of Pop-III star formation suggest that their masses may be limited to $\lesssim 40 M_{\odot}$ due to radiative feedback effects (Hosokawa et al. 2011), which would be in accord with our choice of the the maximum mass for Pop-III stars.

We also plot the data compiled by Hopkins (2004); Pascale et al. (2009); Rodighiero et al. (2010); Karim et al. (2011); Cucciati et al. (2012), that deduced from LBGs, (Ouchi et al. 2004; Bouwens et al. 2007; Mannucci et al. 2007; Verma et al. 2007; Bouwens et al. 2008, 2011b), and that inferred from GRBs (Yüksel et al. 2008; Kistler et al. 2009). Above $z > 4$, each LBG data points are obtained by integrating its LF down to a certain limiting luminosity which is parameterized by the characteristic luminosity L_* of the LF. We note that different authors choose different limiting luminosities. Our model shows the star formation in all galaxies, down to the faintest luminosities.

There is an apparent discrepancy between our model and the observed CSFH data at $1 < z < 5$. In our semi-analytical model, we directly estimate the star formation rate in a galaxy and evaluate the CSFH by integrating the star formation rates of all galaxies. Since the CSFH data are converted from the observed galaxy LFs, there are following observational uncertainties: faint-end slope of the LF, dust obscuration correction from UV data, contamination from old stellar populations to the IR luminosity, total IR luminosity modeling, and a conversion factor from luminosity to star formation rate. In the case of Hopkins (2004); Hopkins & Beacom (2006) CSFH model, there are inconsistencies with other observational information such as stellar mass density (e.g. Choi & Nagamine 2012) and core collapse supernovae rate (Horiuchi et al. 2011). Recently, Kobayashi et al. (2012) have shown that this discrepancy is due to the overcorrection of dust obscuration and star formation rate conversion. These uncertainties will result a factor of $\sim 2-3$ overestimation of CSFH (Kobayashi et al. 2012). Therefore, the discrepancy does not adversely affects our results, since our model can reproduce various observations for galaxies.

2.2. Stellar and Dust Emission

We calculate the emissivity of the Universe at a given redshift from the CSFH that is given as a function of metallicity and the dust attenuation strength using stellar population synthesis models. We use stellar population synthesis models of Schaerer (2003) for $Z < 10^{-4}$ (Pop-III) and Bruzual & Charlot (2003) for $Z \geq 10^{-4}$ to calculate the stellar emissivity. Although Bruzual & Charlot (2003) is commonly used and cover a wide range of metallicity, the $Z < 10^{-4}$ population is not included. Schaerer (2003) can evaluate the stellar population evolution at $Z < 10^{-4}$. For dust attenuation

² We adopt $Z_{\odot} \simeq 0.02$ (Anders & Grevesse 1989; Grevesse & Sauval 1998). However, Asplund et al. (2009) updated the value of $Z_{\odot} \simeq 0.0134$.

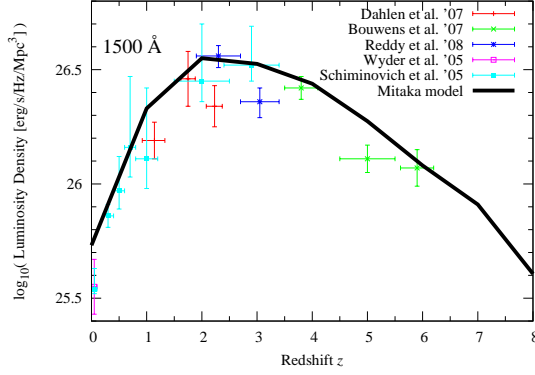


FIG. 2.— Luminosity density at 1500 Å. Solid line is the Mitaka model. The observed data at various redshifts are also shown as indicated in the figure (Wyder et al. 2005; Schiminovich et al. 2005; Dahlen et al. 2007; Bouwens et al. 2007; Reddy et al. 2008).

in galaxies and the intergalactic medium (IGM), we adopt Calzetti et al. (2000) and Yoshii & Peterson (1994), respectively.

Various instruments have constrained the UV LD up to $z \sim 6$ (Wyder et al. 2005; Schiminovich et al. 2005; Dahlen et al. 2007; Bouwens et al. 2007; Reddy et al. 2008). Fig. 2 compares the UV LD from our model with observed LD data at a rest-frame of 1500 Å. All the data agree well with our semi-analytical model. Comparison with other kinds of data are shown in Nagashima & Yoshii (2004); Nagashima et al. (2005); Kobayashi et al. (2007, 2010).

Dust emits mid-IR (MIR) and FIR photons by reemitting the absorbed starlight. For dust emission, we also utilize the Mitaka model (see Makiya et al. in preparation, for details). We set the total IR emissivity is equivalent to the total absorbed starlight energy by dust. Although our IR emissivity model can reproduce the local *Herschel* galaxy luminosity function (Vaccari et al. 2010), the redshift evolution of IR luminosity function (e.g. Rodighiero et al. 2010) has not been reproduced yet (Makiya et al. in preparation). Thus, we predict an IR EBL at $z = 0$ that is than limit of the EBL by a factor of two. To avoid this, we set our IR emissivity model three times more luminous than the usual version of the Mitaka model. Our IR model prediction at MIR–FIR is uncertain, while our model is accurate at the UV–NIR band. We also note that gamma-ray opacity generated by dust emission is effective only above several tens TeV (see Eq. 1).

For the IR spectrum template, we use the Dale & Helou (2002) dust emission model. In their model, the IR spectral energy distribution (SED) shape is defined by the exponent α of Eq. 1 in Dale & Helou (2002). We adopt $\alpha = 1.2$ for all galaxies in our model to reproduce the peak wavelength of the FIR EBL. When we use a different α parameter, the position of the FIR peak wavelength will change.

3. COSMIC REIONIZATION HISTORY

Cosmic reionization is a major change in the ionization state of the Universe. After the recombination epoch, the Universe was in the dark age where no radiation sources existed. As dark matter halos evolved from the first small inhomogeneities in matter density field, some of baryons started to fall in the dark matter halo potential well. When the mass of the halo is high enough, the fallen gas formed stars and galaxies. The first population of stars and galaxies can generate the

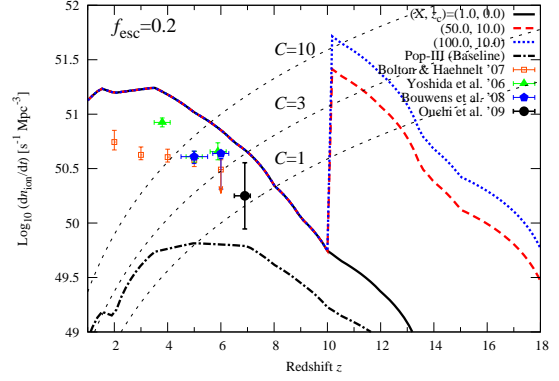


FIG. 3.— Ionizing photon emissivity per comoving Mpc^3 , dn_{ion}/dt , as a function of redshift. We set $f_{\text{esc}} = 0.2$ for all models and observed data. Solid, dashed, and dotted curve shows the baseline, the lower-Pop-III, the upper-Pop-III model, respectively. Dot-dashed curve shows the ionizing photon emissivity from Pop-III population in the baseline model. The filled symbol shows the data derived from galaxy UV LFs (Yoshida et al. 2006; Bouwens et al. 2008; Ouchi et al. 2009). The data derived from the combination of hydrodynamical simulations and $\text{Ly}\alpha$ forest opacity (Bolton & Haehnelt 2007) are shown by open symbols. Thin dashed lines plot the model predictions of the ionizing photon emissivity that is required for maintaining hydrogen ionization in IGM (Madau et al. 1999) with clumping factors of $C = 1, 3$, and 10 , from bottom to top.

UV radiation. This radiation would ionize the Universe (see Barkana & Loeb 2001, for reviews). In this section, we follow the reionization history of the Universe with our Mitaka model.

3.1. Ionizing Photon Emission Rate

The emission rate of hydrogen ionizing photon is required to follow the cosmic reionization history. Hereafter, we take the escape fraction of ionizing photons from a galaxy f_{esc} at all redshift to be 0.2 motivated by the numerical simulations of Yajima et al. (2009, 2011). They also showed that f_{esc} depends on halo mass. Although $f_{\text{esc}} \simeq 0.05$ is found in LBGs at $z \sim 3$ (Shapley et al. 2006; Iwata et al. 2009), the escape fraction of ionizing photons at $z \geq 4$ has not been observationally determined yet. Ono et al. (2010) put an upper limit on f_{esc} at high redshift as $f_{\text{esc}} \lesssim 0.6$ at $z = 5.7$ and $f_{\text{esc}} \lesssim 0.9$ at $z = 6.6$.

Fig. 3 shows the ionizing photon emissivity, dn_{ion}/dt , in the unit of $1/\text{s}/\text{Mpc}^3$ comparing with various observations. We set $f_{\text{esc}} = 0.2$ for all the observed data as well. The observed ionizing photons are derived from galaxy UV LFs at $z = 4 - 7$ (Yoshida et al. 2006; Bouwens et al. 2008; Ouchi et al. 2009, filled symbols in Fig. 3) by Ouchi et al. (2009). The conversion from LF to ionizing photon emissivity is based on the Eq. 5 in Ouchi et al. (2009), where continuous star formation history is assumed for all galaxies. The data are integrated down to $L = 0$. We also show the ionizing photon rate inferred from the $\text{Ly}\alpha$ forest (Bolton & Haehnelt 2007, open symbols in Fig. 3), which is derived by combining hydrodynamical simulations with measurements of the $\text{Ly}\alpha$ opacity of the IGM.

As shown later, the baseline Mitaka model does not produce enough ionizing photons for the measured Thomson scattering optical depth, although it can produce sufficient ionizing photons to reionize the Universe at $z \lesssim 8$. We introduce two parameters to make it consistent with various reionization data. One is the normalization factor X which renormalize the ionizing photon emissivity by a factor of X and the other is the normalizing redshift z_c where

we renormalize the ionizing photon emissivity by a factor of X only at $z > z_c$ from the baseline Mitaka model. In Fig. 3, we show models with $(X, z_c) = (1.0, 0.0)$ (baseline model), $(50.0, 10.0)$, and $(100.0, 10.0)$. Hereafter, we name $(X, z_c) = (1.0, 0.0)$, $(50.0, 10.0)$, and $(100.0, 10.0)$ model as the baseline model, the lower-Pop-III model, and the upper-Pop-III model, respectively. Fig. 3 shows the contribution of Pop-III stars in the baseline model.

Although the overall behavior of our ionizing photon emissivity model at $2 < z < 7$ is similar to that of the observed data, we overestimate the ionizing photon emissivity about a factor of 2 comparing to the data. We note that the observed data are very sensitive to the assumed spectral index of ionizing emission α (see Eq. 5 in Ouchi et al. 2009) which is not well determined. α is set to be 3.0 for the data in the Fig. 3. Once we set $\alpha = 1.5$, it will double the data derived from the galaxy UV LF and the Ly α forest opacity.

Fig. 3 also shows the required dN_{ion}/dt to balance recombination of hydrogen IGM based on the model of Madau et al. (1999),

$$\frac{dn_{\text{ion}}}{dt} = \frac{n_{\text{H}}^0}{t_{\text{rec}}(z)} \simeq 10^{47.4} C(1+z)^3 [\text{s}^{-1} \text{Mpc}^{-3}] \quad (2)$$

where n_{H}^0 is the number density of hydrogens at present-day, $t_{\text{rec}}(z)$ is the recombination time scale at z , and $C = \langle n_{\text{H}}^2 \rangle / \bar{n}_{\text{H}}^2$ is a time dependent volume-averaged clumping factor. We show the cases of $C = 1, 3$, and 10 . $C = 1$ corresponds to the homogeneous Universe. Each of our models predict that there was a sufficient ionizing photon energy budget to ionize the Universe at $z \leq 7-8$ depending on C . However, the baseline model can not ionize the Universe before the epoch of $z = 8$. If the Universe is reionized instantaneously, it might be occurred at $z = 10.6 \pm 1.2$ inferred from the WMAP data (Komatsu et al. 2011). Even if the cosmic reionization is not instantaneous, we may need more ionizing photons above $z \sim 8$ than the ionizing photon emissivity limit by Madau et al. (1999).

3.2. Probing the Cosmic Reionization History

Important indicators of the reionization history are the Thomson electron scattering optical depth and the neutral fraction of hydrogens. Following Barkana & Loeb (2001), we compute the reionization history of the Universe. The ionization equilibrium equation in terms of volume filling factor of HII region Q_{HII} is given as

$$\frac{dQ_{\text{HII}}}{dt} = \frac{1}{n_{\text{H}}^0} \frac{dn_{\text{ion}}}{dt} - \alpha_B \frac{C}{a(t)^3} n_{\text{H}}^0 Q_{\text{HII}}, \quad (3)$$

where t is the cosmic time, $n_{\text{H}}^0 = X_{\text{H}} n_{\text{B}}^0$ is the number density of hydrogen at present-day, n_{B}^0 is the number density of baryons at present-day, and $X_{\text{H}} = 0.76$ is the hydrogen mass fraction, dn_{ion}/dt is the ionizing photon production rate (see Fig. 3), $\alpha_B = 2.6 \times 10^{-13} \text{ cm}^3 \text{ s}^{-1}$ is the hydrogen recombination rate, and $a(t)$ is the scale factor. The recombination time scale $t_{\text{rec}}(z)$ in Eq. 2 is given as $a(t)^3 / \alpha_B C n_{\text{H}}^0$.

Equation 3 is solved as (see Barkana & Loeb 2001, for details)

$$Q_{\text{HII}}(z_0) = \int_{z_0}^{\infty} dz \left| \frac{dt}{dz} \right| \frac{1}{n_{\text{H}}^0} \frac{dn_{\text{ion}}}{dt} e^{F(z, z_0)}, \quad (4)$$

where a constant C is assumed and dt/dz is calculated by the Friedmann equation in the standard flat universe cosmology

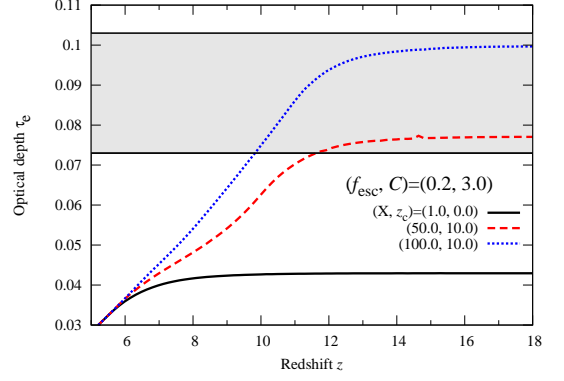


FIG. 4.— Thomson scattering optical depth of the Universe. We set $f_{\text{esc}} = 0.2$ and $C = 3.0$. Solid, dashed, and dotted curve corresponds to the baseline, the lower-Pop-III, and the upper-Pop-III model, respectively. Shaded region shows the 7-year WMAP results with $1-\sigma$ errors $\tau_e = 0.088 \pm 0.015$ (Komatsu et al. 2011).

as

$$\frac{dt}{dz} = \frac{1}{(1+z)H_0 \sqrt{\Omega_M(1+z)^3 + \Omega_\Lambda}}. \quad (5)$$

Once Q_{HII} reaches 1, there is no neutral hydrogens and ionizing photons are saved in the intergalactic space. The function $F(z, z_0)$ takes into account of recombination and given as

$$F(z, z_0) = -\frac{2}{3} \frac{\alpha_B n_{\text{H}}^0}{\sqrt{\Omega_M} H_0} C [f(z) - f(z_0)], \quad (6)$$

where $f(z)$ is defined as

$$f(z) = \sqrt{(1+z)^3 + \frac{1-\Omega_M}{\Omega_M}}. \quad (7)$$

In this paper, we set $C = 3.0$ motivated by Pawlik et al. (2009). We do not change C as a function of redshift. We also assume $Q_{\text{HeII}} = Q_{\text{HII}}$ and neglecting the electron populations from Q_{HeIII} region to compute the optical depth of electron scattering. Then, the number density of free electrons at z is written as

$$\begin{aligned} n_e(z) &= \left(Q_{\text{HII}}(z) X_{\text{H}} + \frac{Q_{\text{HeII}}(1-X_{\text{H}})}{4} \right) n_{\text{B}}^0 (1+z)^3 \\ &= \frac{1+3X_{\text{H}}}{4} Q_{\text{HII}}(z) n_{\text{B}}^0 (1+z)^3. \end{aligned} \quad (8)$$

The optical depth to the Thomson electron scattering is

$$\tau_e(z_0) = \int_0^{z_0} dz \frac{dl}{dz} \sigma_T n_e(z), \quad (9)$$

where σ_T is the Thomson cross section and dl/dz is the cosmological line element given as

$$\frac{dl}{dz} = c \frac{dt}{dz} = \frac{c}{(1+z)H_0 \sqrt{\Omega_M(1+z)^3 + \Omega_\Lambda}} \quad (10)$$

for a standard flat universe cosmology.

Fig. 4 shows the Thomson scattering optical depth of the Universe. We also show the 7-year WMAP data which reports $\tau_e = 0.088 \pm 0.015$ (Komatsu et al. 2011). The baseline model can not reproduce the WMAP data due to the insufficient ionizing photons at $z > 8$ (see Fig. 3), although it can reionize the Universe at $z \lesssim 8$. The lower-Pop-III and upper-Pop-III model

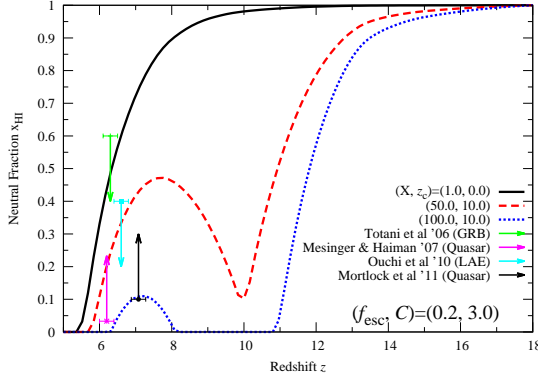


FIG. 5.— Hydrogen neutral fraction of the Universe. We set $f_{\text{esc}} = 0.2$ and $C = 3.0$. Solid, dashed, and dotted curve corresponds to the baseline, the lower-Pop-III, and the upper-Pop-III model, respectively. We also show Gunn-Peterson trough test constraints on the neutral fraction from quasars (Mesinger & Haiman 2007; Mortlock et al. 2011), a GRB (Totani et al. 2006), and LAEs (Ouchi et al. 2010).

reproduces the lower-limit and upper-limit of the *WMAP* data, respectively. Therefore, we need 50-100 times more ionizing photons at $z > 10$ to be consistent with the *WMAP* Thomson scattering optical depth measurement than those naturally expected from a semi-analytical galaxy formation model.

Fig. 5 shows the hydrogen neutral fraction of the Universe, $x_{\text{HI}} = 1 - Q_{\text{HI}}$. Gunn-Peterson trough test constraints (Gunn & Peterson 1965) from quasars (Mesinger & Haiman 2007; Mortlock et al. 2011), a GRB (Totani et al. 2006), and LAEs (Ouchi et al. 2010) are also shown. We do not show the constraints from quasars at $z \lesssim 6$ (e.g. Fan et al. 2006). This is because we do not include the neutral hydrogen distribution which is not observationally well understood. However, this does not affect our argument, since we trace the global reionization history. We note that the neutral hydrogen distribution is important to trace the ionization state of small scale structures.

As shown in Fig. 5, the three models well trace the history of the neutral fraction of the Universe. Since we renormalize the ionizing photon emissivity above z_c for the lower-Pop-III model and the upper-Pop-III model, ionizing photon emissivity suddenly decreases at $z = z_c$ and the Universe starts to recombine ionized hydrogens again. This is because these two models show a bump feature at $z \sim 7$.

As shown in Figs. 4 and 5, 50–100 times more ionizing photons are required at $z > 10$ to be consistent with the Thomson scattering optical depth measurement comparing to the baseline model which successfully reproduces the various observational data of galaxy formation and generates sufficient ionizing photons to reionize the Universe at $z \lesssim 8$. Observationally, it is also known that the estimates of the Thomson optical depths and contribution of galaxies to reionization are higher than those in observational studies of galaxies detected at $z \lesssim 8$ (e.g. Stark et al. 2007; Chary 2008; Oesch et al. 2009; Ouchi et al. 2009; Pawlik et al. 2009; Bunker et al. 2010; Labbé et al. 2010; Robertson 2010; Bouwens et al. 2011a, 2012). The enhancement of ionizing photon emissivity might be required at high redshift to be consistent with the *WMAP* measurement of the Thomson scattering optical depth.

There are various possible ingredients which play an important role in generating sufficient ionizing photons for the *WMAP* data. These are the steeping of the faint-end slope index of LF (Bouwens et al. 2012), a smaller clumping factor

(Bolton & Haehnelt 2007; Pawlik et al. 2009), a larger escape fraction (Yajima et al. 2011), a harder initial mass function at higher redshift (McKee & Tan 2008), a contribution from early Pop-III stars (Cen 2003), and feedback from accreting black holes (Ricotti & Ostriker 2004; Mirabel et al. 2011).

To study Pop-III stars' contribution to the NIR background, we assume that required ionizing photon comes from Pop-III stars. This assumption will maximize the Pop-III stars' contribution to the NIR background. Therefore, we renormalize the Pop-III emissivity by a factor of X at $z > z_c$. As shown later, this does not significantly affect our EBL and gamma-ray optical depth models.

4. EXTRAGALACTIC BACKGROUND LIGHT

We compute the background intensity $I(\nu_0, z_0)$ at redshift z_0 and frequency ν_0 which is the integrated radiation from all sources between $z = z_0$ and the maximum redshift of the source distribution, z_{max} . Their contribution to the local background intensity is given by (see e.g. Peacock 1999)

$$I(\nu_0, z_0) = \frac{1}{4\pi} \int_{z_0}^{z_{\text{max}}} dz \frac{dl}{dz} j(\nu, z), \quad (11)$$

where $j(\nu, z)$ is the galaxy comoving volume emissivity at redshift z and frequency $\nu = \nu_0(1+z)$. We set $z_{\text{max}} = 20$. The galaxy comoving volume emissivity is calculated by combining our CSFH and stellar population synthesis models.

For the units in the proper volume, from Eq. 11, the specific radiation energy density (in the unit of $\text{erg/s/cm}^3/\text{Hz}$) in the proper volume is

$$\rho(\nu_0, z_0) = \frac{4\pi}{c} (1+z_0)^3 I(\nu_0, z_0) \quad (12)$$

where a factor of $(1+z_0)^3$ corrects the energy density from local to z_0 . The photon proper number density is

$$\frac{dn(\epsilon_0, z_0)}{d\epsilon_0} = \frac{\rho(\nu_0, z_0)}{\epsilon_0}, \quad (13)$$

where $\epsilon_0 = h_p \nu_0$ is the photon energy and h_p is the Planck constant.

Fig. 6 shows plots of the proper photon number density based on the baseline, upper-Pop-III, and lower-Pop-III models. When we increase the Pop-III population, we increase their stellar radiation only. Thus, there is a discontinuity at ~ 0.2 eV ($\sim 6.2 \mu\text{m}$). Proper photon number density increases from high redshift to $z \sim 1-3$ where the CSFH has a peak and decreases toward the local Universe. Once we increase the Pop-III component, the UV photon density at high redshift becomes comparable to that at $z = 1$.

The local background intensity reported in Fig. 7 as a function of wavelength λ is calculated from Equation 11 by setting $z_0 = 0$. We show the baseline model here. We also show other theoretical models for the comparison (Kneiske et al. 2004; Stecker et al. 2006; Franceschini et al. 2008; Gilmore et al. 2009; Finke et al. 2010; Kneiske & Dole 2010; Gilmore et al. 2012). The current measurements of the EBL and the integrated brightness of galaxies are also shown. Detailed predictions for the proper photon number density and the local background intensity is publicly distributed on the Web site <http://www.slac.stanford.edu/~yinoue/Download.htm>

Overall shape of our EBL model is consistent with the observational data. Our model is in a good agreement with the observations by *Pioneer 10/11* (Matsuoka et al. 2011, open

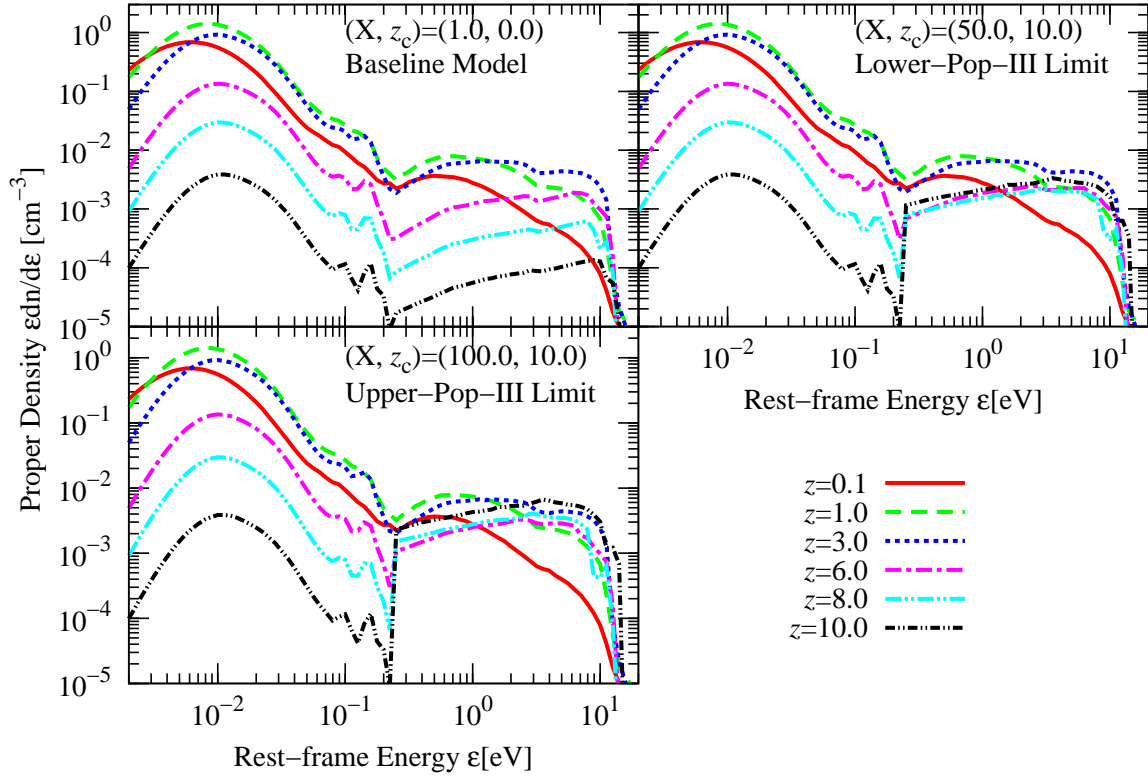


FIG. 6.— Proper volume photon number densities multiplied by the photon energy ϵ as a function of redshift. Top-left, top-right, and bottom-left panel corresponds to the baseline model, the upper-Pop-III model, and the lower-Pop-III model, respectively. For the upper-Pop-III and lower-Pop-III models, we only renormalize their stellar contribution. Solid, dashed, dotted, dot-dashed, double dot-dashed, and triple dot-dashed curve corresponds to the proper photon density at $z = 0.1, 1.0, 3.0, 6.0, 8.0$, and 10.0 , respectively.

pentagon symbols in Fig. 7) which directly measured the EBL from the outside of the zodiacal region. Our model also does not violate the limit from the gamma-ray observation (Albert et al. 2008).

Comparing to other models, we tends to predict more photons at $\lambda \leq 0.4\mu\text{m}$ and less photons at $\lambda > 0.4\mu\text{m}$. At UV range, other models except for Stecker et al. (2006) are consistent with the *GALEX* data (Xu et al. 2005), while ours are consistent with the *HST* data (Gardner et al. 2000). Both observational data points show the integrated galaxy counts down to zero luminosity. The reason why we predict more UV photons is due to the treatment of the dust obscuration. Somerville et al. (2012) showed that a model with the Calzetti law (Calzetti et al. 2000), which we adopt, predicts more UV photons comparing to models with the multi-dust component model which Gilmore et al. (2012); Somerville et al. (2012) adopted. We also note that the data points by Madau & Pozzetti (2000) are the integrated galaxy counts down to the detection limit of the *HST*. Therefore, Madau & Pozzetti (2000) gives the lower-limit of the EBL.

At $0.4\mu\text{m} < \lambda < 10\mu\text{m}$, our model is reasonably in a good agreement with Kneiske & Dole (2010) which predict the lower-limit of the EBL. The reason why we predict less photons at $\lambda > 0.4\mu\text{m}$ comparing to other models is that our CSFH is a factor of 3 lower than that of Hopkins & Beacom (2006) which are used in most of previous studies.

Fig. 8 shows the Pop-III EBL from the baseline, upper-Pop-III, and lower-Pop-III models. Each model shows the Pop-III contribution is $\leq 0.03 \text{ nW/m}^2/\text{sr}$ which is less than

0.5% of the total NIR background radiation. It is difficult to explain the *IRTS* data (Matsumoto et al. 2005) by the Pop-III population even with the highest level of the arrowed Pop-III contribution from the reionization constraints. Moreover, even if the trapped ionizing photons in a galaxy is converted to Ly- α photons, the NIR flux from Pop-III stars will increase only 15% in the case B recombination. Therefore, it is hard to extract the Pop-III star information from the NIR background flux measurements. Since we renormalize the Pop-III population at $z > z_c = 10$, two peaks appear in the upper-Pop-III EBL and the lower-Pop-III EBL.

5. GAMMA-RAY ATTENUATION

5.1. Gamma-ray Opacity

The redshift dependent background photon number density is now obtained by following §4. We are able to compute the gamma-ray opacity for pair production interactions. The cross section of pair production process is given as (Heitler 1954)

$$\sigma_{\gamma\gamma}(E_\gamma, \epsilon, \theta) = \frac{3\sigma_T}{16} (1 - \beta^2) \times \left[2\beta(\beta^2 - 2) + (3 - \beta^4) \ln \left(\frac{1 + \beta}{1 - \beta} \right) \right], \quad (14)$$

where ϵ is the energy of the background photon, E_γ is the energy of colliding high energy photon, θ is the angle between

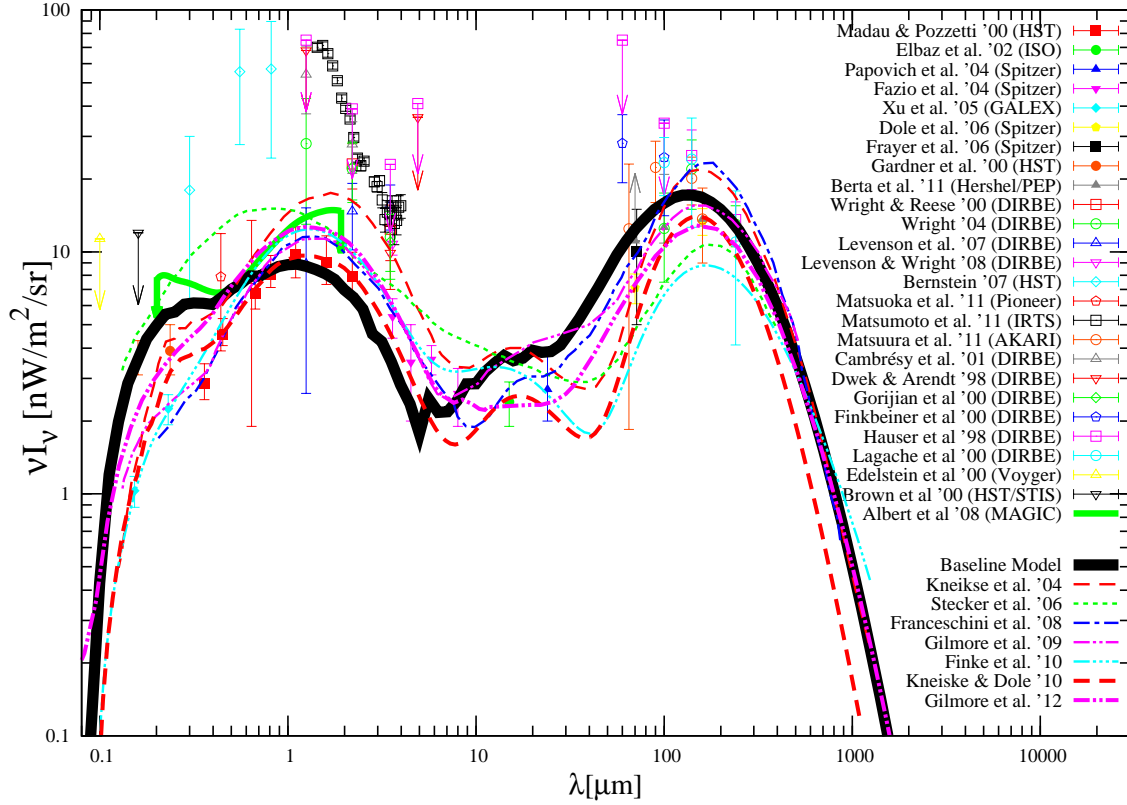


FIG. 7.— The EBL model for the baseline model is shown by solid curve. For comparison, the EBL models by Kneiske et al. (2004, thin dashed), Stecker et al. (2006, dotted), Franceschini et al. (2008, dot-dashed), Gilmore et al. (2009, thin double dot-dashed), Finke et al. (2010, triple dot-dashed), Kneiske & Dole (2010, thick dashed), and Gilmore et al. (2012, thick double dot-dashed) are shown as indicated in the figure. The integrated brightness of galaxies (minimum EBL; filled symbols) and current measurements of the EBL (open symbols) are shown as indicated in the figure. References for the integrated brightness of galaxies are *HST* (Madau & Pozzetti 2000; Gardner et al. 2000), *ISO* (Elbaz et al. 2002), *Spitzer* (Papovich et al. 2004; Fazio et al. 2004; Dole et al. 2006; Frayer et al. 2006), *GALEX* (Xu et al. 2005), and *Herschel* (Berta et al. 2011). References for the current EBL measurements are *DIRBE* (Wright & Reese 2000; Wright 2004; Levenson et al. 2007; Levenson & Wright 2008; Cambr  s et al. 2001; Dwek & Arendt 1998; Gorjian et al. 2000; Finkbeiner et al. 2000; Hauser et al. 1998; Lagache et al. 2000), *HST* (Bernstein 2007; Brown et al. 2000), *Pioneer* (Matsuoka et al. 2011), *IRTS* (Matsumoto et al. 2005), *AKARI* (Matsuura et al. 2011), and *Voyager* (Edelstein et al. 2000). The upper limit from TeV gamma-ray observation by MAGIC (Albert et al. 2008) is also shown by solid line with arrows.

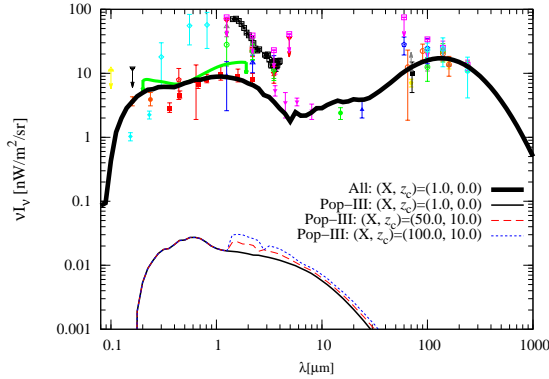


FIG. 8.— Same as Fig. 7, but showing the Pop-III contribution to the EBL. Thick solid curve shows the total EBL. Thin-solid, dashed, and dotted curve corresponds to the baseline, the upper-Pop-III and the lower-Pop-III model, respectively.

the colliding photons, and β is

$$\beta \equiv \sqrt{1 - \frac{2m_e^2 c^4}{\epsilon E_\gamma (1 - \cos\theta)}}; \quad \mu \equiv \cos\theta. \quad (15)$$

Then, the gamma-ray opacity is maximized for photon energy is as shown in Eq. 1.

The optical depth for a high energy photon E_γ propagating the universe from a source at redshift z_s to an observer at z_0 is

$$\tau_{\gamma\gamma}(E_\gamma, z_s) = \int_{z_0}^{z_s} dz \int_{-1}^1 d\mu \int_{\epsilon_{th}}^\infty d\epsilon \frac{dl}{dz} \frac{1-\mu}{2} \times \frac{dn(\epsilon, z)}{d\epsilon} \sigma_{\gamma\gamma}(E_\gamma(1+z), \epsilon, \theta), \quad (16)$$

where ϵ_{th} is the threshold energy for pair production process and given as

$$\epsilon_{th} = \frac{2m_e^2 c^4}{E_\gamma(1+z)(1-\mu)}. \quad (17)$$

Fig. 9 shows the optical depth for $\gamma\gamma$ interaction as a function of the observed gamma-ray energy E_γ from $z = 0 - 10$ comparing with various previous models (Kneiske et al. 2004; Franceschini et al. 2008; Finke et al. 2010; Gilmore et al. 2012; Inoue et al. 2010a). We calculate it using Eq. 16 by setting $z_0 = 0$, while the model by Inoue et al. (2010a) has set $z_0 = 4$. We have not considered the absorption by the CMB photons which is negligible in the parameter range of our interest at 1 GeV – 100 TeV. We show here the baseline model only, since the Pop-III contribution is negligible (see

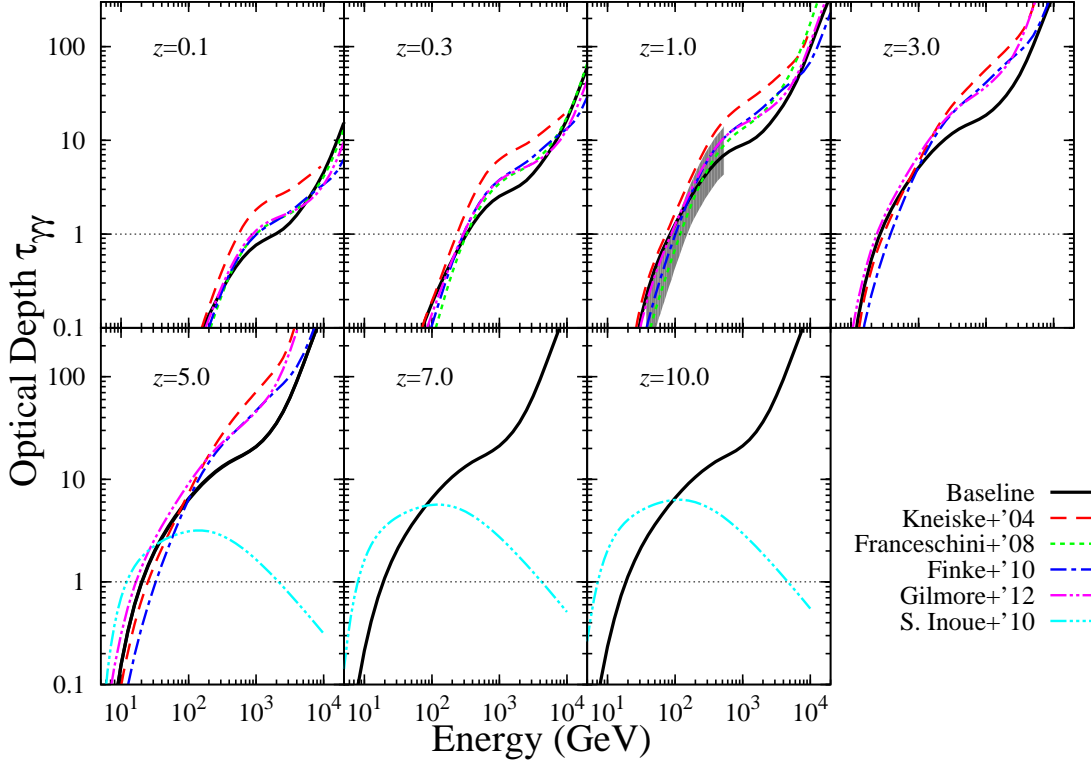


FIG. 9.— Gamma-ray optical depth for the observed gamma-ray energy E_γ from $z = 0.1, 0.3, 1.0, 3.0, 5.0, 7.0$, and 10.0 . Solid curve shows the baseline model which is comparable to other models in this paper. Dashed, dotted, dot-dashed, double dot-dashed, triple dot-dashed curve shows the model by Kneiske et al. (2004) Franceschini et al. (2008), Finke et al. (2010), Gilmore et al. (2012), and Inoue et al. (2010a), respectively. Shaded region represents the measurement at the 95% confidence level of the gamma-ray opacity by *Fermi* at $z \approx 1$ (The *Fermi*-LAT Collaboration 2012). Horizontal thin dotted line shows $\tau_{\gamma\gamma} = 1$. Since the difference among models with various Pop-III contents is small, we do not plot other models in this paper.

below and §. 4). Detailed predictions for the $\gamma\gamma$ optical depth based on our model is publicly distributed on the Web site <http://www.slac.stanford.edu/~yinoue/Download>.

Our gamma-ray opacity model is consistent with the gamma-ray opacity measurement by *Fermi* at $z \approx 1$ at the 95% confidence level (The *Fermi*-LAT Collaboration 2012). Our model is also generally consistent with previous models (Kneiske et al. 2004; Franceschini et al. 2008; Finke et al. 2010; Gilmore et al. 2012) at $E_\gamma \lesssim 400/(1+z)$ GeV at $z \leq 5$. However, opacity above $E_\gamma \sim 400/(1+z)$ GeV is a factor of ~ 2 transparent to previous models. We predict low EBL intensity at $\lambda > 0.4 \mu\text{m}$ (see Fig. 7) where the gamma-ray opacity is maximized for the ~ 300 GeV photons (see Eq. 1).

As we described before, redshift evolution of our MIR–FIR emissivity model is uncertain. EBL with longer than MIR is important for the absorption of gamma-rays above several tens TeV following Eq. 1. Therefore, this uncertainty would not affect to our results below 10 TeV.

We predict higher energy cut-off in the gamma-ray spectrum at ~ 20 GeV for sources at $z \gtrsim 6$ comparing to that in Inoue et al. (2010a) which predicted ~ 12 GeV at $z \sim 5$ and ~ 6 – 8 GeV at $z \gtrsim 8$ – 10 . This is because the UV radiation from Pop-III stars are not sufficient enough to significantly absorb gamma-rays at high redshift even in the case of the upper-Pop-III model as discussed below. Since path length at $z \gtrsim 6$ is not so long as that at lower redshift, the high emissivity due to Pop-III stars does not affect the opacity significantly.

By setting $z_c = 10$, our model predicts few UV photons below $z = 10$ to keep reionization, while Inoue et al. (2010a) has kept sufficient UV photons at $z < 10$. Moreover, Inoue et al. (2010a) did not include stars with metallicity higher than $Z = 0.02Z_\odot$. These might be the main reason why our predictions are different. We note that the EBL contribution from quasars which is not included in our study is not significant as shown in Inoue et al. (2010a).

Based on a gamma-ray luminosity function of blazars, *Fermi* is expected to detect a blazars at $z \sim 6$ (Inoue et al. 2011). Moreover, GRBs are also promising as they are known to occur at $z > 6$ (Kawai et al. 2006; Greiner et al. 2009), at least up to $z \sim 8.2$ (Tanvir et al. 2009), and probably out to the epoch of first star formation in the Universe (Bromm & Loeb 2006). For example, if a GRB 080916C-like event (Abdo et al. 2009) is occurred at $z \sim 6$ which was the brightest GRB event in the gamma-ray sky, CTA can clearly detect its gamma-ray spectrum (Inoue et al. in preparation).

Fig. 10 shows the $\gamma\gamma$ opacity from all stars, Population I (Pop-I) stars ($10^{-2.5} \leq Z$), Pop-II stars ($10^{-4} \leq Z < 10^{-2.5}$), and Pop-III stars ($Z < 10^{-4}$). Since the metallicity transition between Pop-II stars (halo stars) and Pop-I stars (disk stars) is $[\text{Fe}/\text{H}] \simeq -1$ (Wheeler et al. 1989; McWilliam 1997; Prochaska et al. 2000) corresponding to $Z \simeq 10^{-2.7} - 10^{-2.3}$, we take $Z = 10^{-2.5}$ for the transition metallicity between these populations in this paper. We show here the baseline model. Although it is difficult to capture the direct signature of Pop-III stars in the gamma-ray spectra of high redshift sources, the

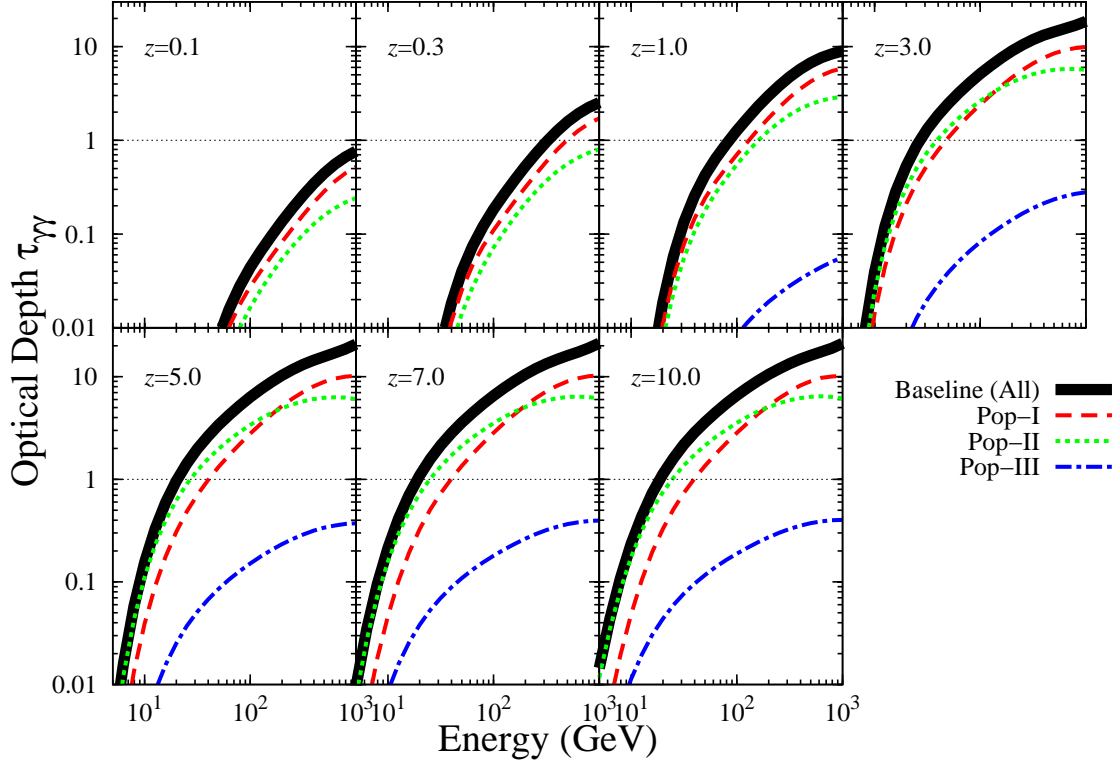


FIG. 10.— Same as Fig. 9, but shows the gamma-ray optical depth from each stellar populations. Solid, dashed, dotted, and dot-dashed curve shows contribution of all stars, Pop-I stars, Pop-II stars, and Pop-III stars, respectively, in the baseline model. Horizontal thin dotted line shows $\tau_{\gamma\gamma} = 1$. Since the contribution of Pop-III stars is weak, it does not appear in the panels at $z = 0.1$ and 0.3 .

attenuation due to Population II stars should be observable in future high- z gamma-ray observation and will provide a valuable probe of the evolving UV EBL in the cosmic reionization epoch. Moreover, once high redshift gamma-ray events are observed, we can at least put an upper limit on the Pop-III stars contribution to the EBL and may be able to distinguish the reionization history of the Universe by comparing our model with Inoue et al. (2010a).

Fig. 11 shows the differential of gamma-ray optical depth $d\tau_{\gamma\gamma}/dz$ with respect to redshift for the baseline, lower-Pop-III, and upper-Pop-III models. Since the Pop-III component is added at $z > 10$, the emissivity contribution from Pop-III is insignificant at $z \lesssim 6$. At $z \gtrsim 6$, the Pop-III contribution to $d\tau_{\gamma\gamma}/dz$ depends on the amount of the Pop-III stars. Therefore, there is a difference in gamma-ray opacity among models at high redshift. This results in $\sim 3\%$, $\sim 10\%$ and $\sim 20\%$ enhancement of the gamma-ray opacity at 20 GeV comparing to the baseline model at $z = 6, 8$, and 10 , respectively. At higher energy, the enhancement decreases. If it is possible to identify $\sim 10\%$ difference in flux, we are able to distinguish our models.

5.2. Comparison with Current GeV & TeV data

Gamma-ray astronomy has now been firmly established by observations of *Fermi*, H.E.S.S., MAGIC, and VERITAS. Further progress is anticipated in the near future by CTA. The most distant gamma-ray object detected in GeV and TeV band is a GRB at $z = 4.35$ (Abdo et al. 2009) and a blazar at $z = 0.536$ (Albert et al. 2008). If the gamma-rays observed from the direction of these sources

are created at the source redshift and are generated by a single component such as shock accelerated particles, the gamma-ray opacity of the Universe has already been constrained (see e.g. Mazin & Raue 2007; Raue & Mazin 2008). CTA is expected to detect > 100 blazars up to $z \sim 2.5$ (Inoue et al. 2010b; Inoue & CTA Consortium 2011; Sol et al. in preparation). Future high redshift blazar observation will be a key to understanding the evolution of the opt.-NIR EBL in detail. Precise low redshift TeV sources observation will be a key to understanding the FIR EBL, since the opacity is huge at high redshift. Although starburst galaxies are suggested as possible targets for the FIR EBL study (Dwek & Krennrich 2012), the internal gamma-ray absorption will not allow photons above 10 TeV escaping from a galaxy (e.g. Inoue 2011b).

A plot of the energy at which the Universe becomes optically thick to gamma-rays, defined where $\tau_{\gamma\gamma} = 1$ is shown in Fig. 12, which is known as the Fazio–Stecker relation (Fazio & Stecker 1970). We show here our baseline model and other models (Kneiske et al. 2004; Franceschini et al. 2008; Finke et al. 2010; Gilmore et al. 2012; Inoue et al. 2010a). Since other models do not compute the opacity at $z = 0 - 10$, we do not show the opacity of each model at the outside of the redshift range of each paper. We also plot the maximum photon energy bins of several blazars (see Finke & Razzaque 2009, for a list and references) and GRB 080916C (Abdo et al. 2009).

Most of blazars are highly attenuated by the EBL, since several sources are considerably above the $\tau_{\gamma\gamma}$ for all models. The highest energy photons from the GRB 080916C constrain

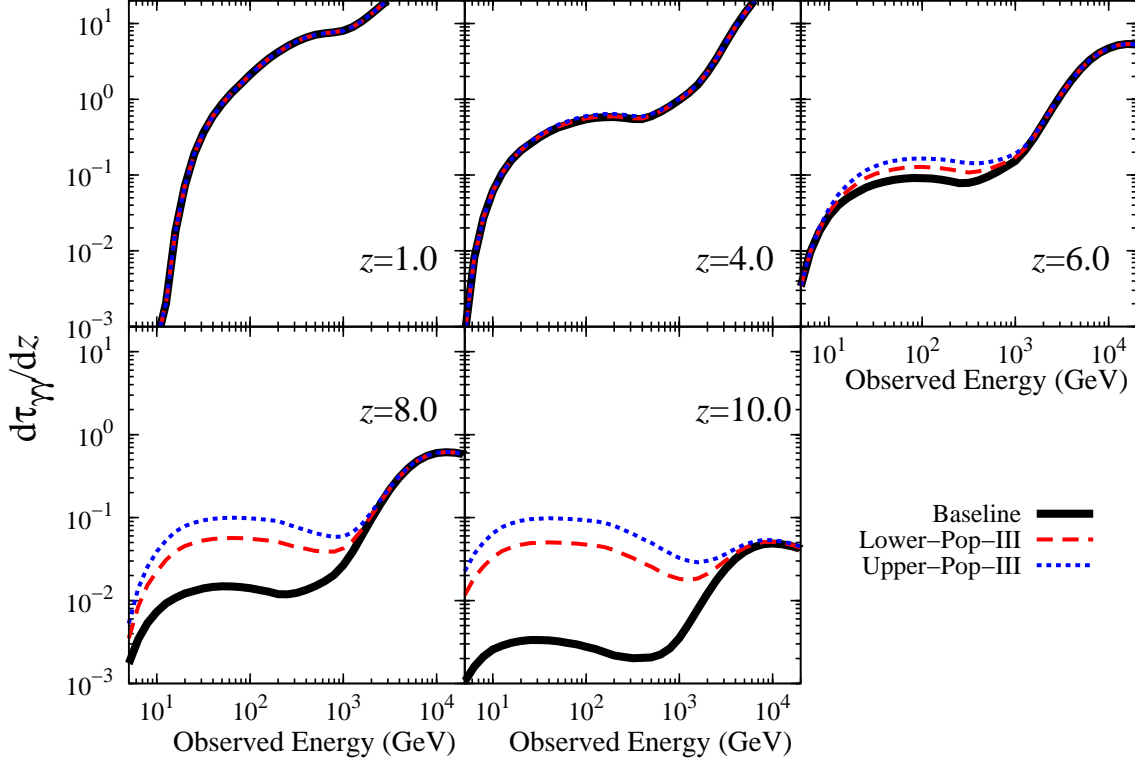


FIG. 11.— Differential of gamma-ray optical depth $d\tau_{\gamma\gamma}/dz$ for the observed gamma-ray energy E_γ with respect to redshift z from $z = 1.0, 4.0, 6.0, 8.0$, and 10.0 . Solid, dashed, and dotted curve shows the baseline, lower-Pop-III, and upper-Pop-III model, respectively. Each curve overlaps each other at $z = 1$ and 4 .

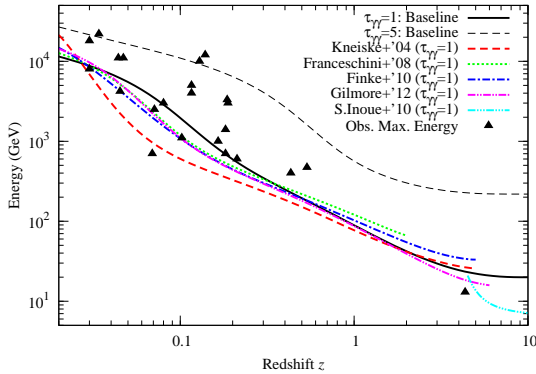


FIG. 12.— Horizon of the Gamma-ray Opacity where $\tau_{\gamma\gamma} = 1$, known as the Fazio-Stecker relation (Fazio & Stecker 1970). The baseline model is shown by solid curve. Dashed, dotted, dot-dashed, double dot-dashed, triple dot-dashed curve shows the model by Kneiske et al. (2004) Franceschini et al. (2008), Finke et al. (2010), Gilmore et al. (2012), and Inoue et al. (2010a), respectively. Thin dashed curve show the case of $\tau_{\gamma\gamma} = 5$ for the baseline model. The filled data points are the observed maximum gamma-ray photon energy bins from blazars (Finke & Razzaque 2009) and the GRB 080916 C (Abdo et al. 2009). Since other papers do not cover the opacity at $z = 0 - 10$, we do not show the opacity of each model at the outside of the redshift range of each paper.

the EBL at high redshifts. Our model predicts that the Universe is transparent below 20 GeV even at $z > 4$.

Figs. 13 and 14 show the observed spectra of TeV blazars at $z \leq 0.15$ and $z > 0.15$, respectively, and their deabsorbed spectra. If TeV emission of these sources are originated from shock accelerated electrons or protons, the intrinsic photon

index $\Gamma_{\text{int}} = 1.5$ is expected to be the hardest in the diffusive shock acceleration (Malkov & O’C Drury 2001). Although the results are generally consistent with a minimum intrinsic $\Gamma_{\text{int}} = 1.5$, some sources such as 1ES 0229-20 and 1ES 1101-232 shows harder spectra. Moreover, it seems that there are two components in some sources, since spectra starts to harden from several hundreds GeV.

Some authors recently claim the existence of the secondary cascade component in these energy band from very high energy cosmic-rays or gamma-rays (e.g. Essey et al. 2011; Essey & Kusenko 2012; Murase et al. 2012; Aharonian et al. 2012). These components will be a key to understanding the IGMFs. Once future CTA observations bring us spectra of these sources with a high energy resolution, we will be able to search such signature by comparing with the deabsorbed blazar spectra.

The EBL absorption signature is not seen in the spectrum of the extragalactic gamma-ray background (EGB) spectrum (Ackermann et al. 2011), although it is naturally expected if the origin is cosmological (Inoue 2011a; Inoue & Ioka 2012). Inoue & Ioka (2012) has recently showed that the EGB measurement at > 100 GeV (Ackermann et al. 2011) violates the EGB itself at < 100 GeV (Abdo et al. 2010) by considering known sources’ contribution. The upper limit on EGB is derived from the cascade emission from EGB above 100 GeV not to exceed the current EGB measurement. Even if our EBL model is adopted, the violation remains. Detailed studies of gamma-ray spectra of extragalactic sources are required to probe this violation.

6. CONCLUSIONS

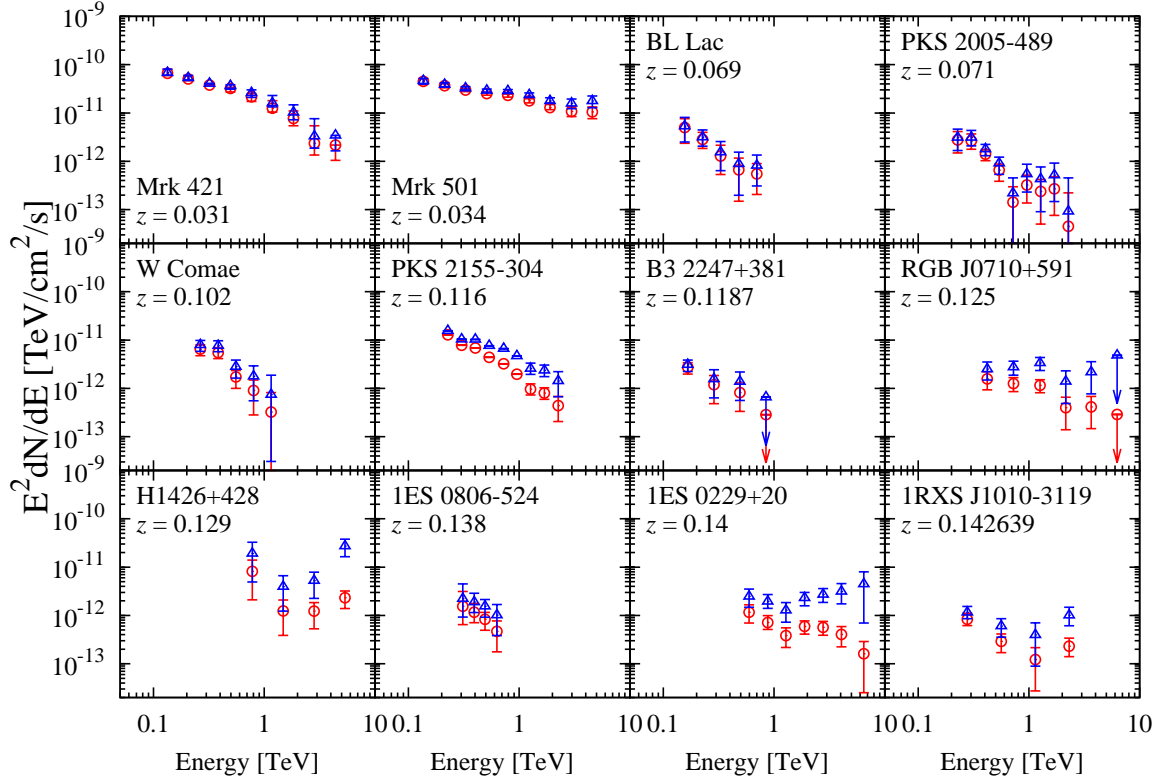


FIG. 13.— TeV Blazar spectra observed (circle) and deabsorbed (triangle) by our baseline model. Sources shown here are at $z \leq 0.15$. References for data are Mrk 421 (Albert et al. 2007c), Mrk 501 (Albert et al. 2007d), BL Lac (Albert et al. 2007a), PKS 2005-489 (Aharonian et al. 2005a), W Comae (Acciari et al. 2008), PKS 2155-304 (Aharonian et al. 2005b), B3 2247+381 (Aleksić et al. 2012), RGB J0710+591 (Acciari et al. 2010), H 1426+428 (Aharonian et al. 2002), 1ES 0806-524 (Acciari et al. 2009a), 1ES 0229+200 (Aharonian et al. 2007c), 1RXS J1010-3119 (Abramowski et al. 2012b).

We have developed models for the EBL over the redshift range $z = 10$ to $z = 0$ on the basis of a semi-analytical model of hierarchical galaxy formation, into which Pop-III stars were incorporated in a simplified fashion. Our baseline model is consistent with a wide variety of observational data for galaxies below $z \sim 6$ (Nagashima & Yoshii 2004; Kobayashi et al. 2007, 2010), and is also capable of reionizing the Universe by $z < 8$. However, in order to account for the Thomson scattering optical depth measured by *WMAP*, the ionizing photon emissivity is required to be 50-100 times higher at $z > 10$. This is line with recent observations of galaxy candidates at $z \sim 8$, as long as the contribution from faint galaxies below the sensitivity of current telescopes is not large (e.g. Bouwens et al. 2012). The “missing” ionizing photons may possibly be supplied by Pop-III stars forming predominantly at these epochs in sufficiently small galaxies.

The EBL intensity at $z = 0$ in our model is generally not far above the lower limits derived from galaxy counts. Our model is also in good agreement with the data from *Pioneer* (Matsuoka et al. 2011) directly measured from outside the zodiacal region. The Pop-III contribution to the NIR EBL is ≤ 0.03 nW/m²/sr, less than 0.5 % of the total in this band, even at the maximum level compatible with *WMAP* measurements. The putative NIR EBL excess (Matsumoto et al. 2005), which also conflicts with the upper limits from gamma-

ray observations (Aharonian et al. 2006a), may have a zodiacal origin rather than Pop-III stars.

Up to $z \sim 3-5$, the $\gamma\gamma$ opacity in our model is comparable to that in the majority of previously published models (Kneiske et al. 2004; Franceschini et al. 2008; Finke et al. 2010; Gilmore et al. 2012) below $E_\gamma \sim 400/(1+z)$ GeV, while it is a factor of ~ 2 lower above this energy. The Universe is predicted to be largely transparent below 20 GeV even at $z > 4$.

Estimates based on the observed gamma-ray luminosity function of blazars show that *Fermi* may detect blazars up to $z \sim 6$ (Inoue et al. 2011). CTA may possibly detect GRBs up to similar redshifts (Inoue et al. in preparation). However, the contribution of Pop-III stars may be difficult to discern in the attenuated spectra of high-redshift gamma-ray sources, even at the highest levels allowed by the *WMAP* constraints. Nevertheless, the signature of Population II stars is expected to be observable in high- z gamma-ray sources, providing a unique and valuable probe of the evolving EBL in the rest-frame UV.

We thank Floyd Stecker and Alberto Dominguez for helpful comments and Tirth Roy Choudhury for providing numerical data from his model. YI acknowledges support by the Research Fellowship of the Japan Society for the Promotion of Science (JSPS). SI is supported by Grants-in-Aid Nos. 22540278 and 24340048 from MEXT of Japan.

REFERENCES

Abdo, A. A. et al. 2009, *Science*, 323, 1688
—, 2010, *Physical Review Letters*, 104, 101101

Abramowski, A. et al. 2012a, arXiv:1201.2044
—, 2012b, ArXiv e-prints

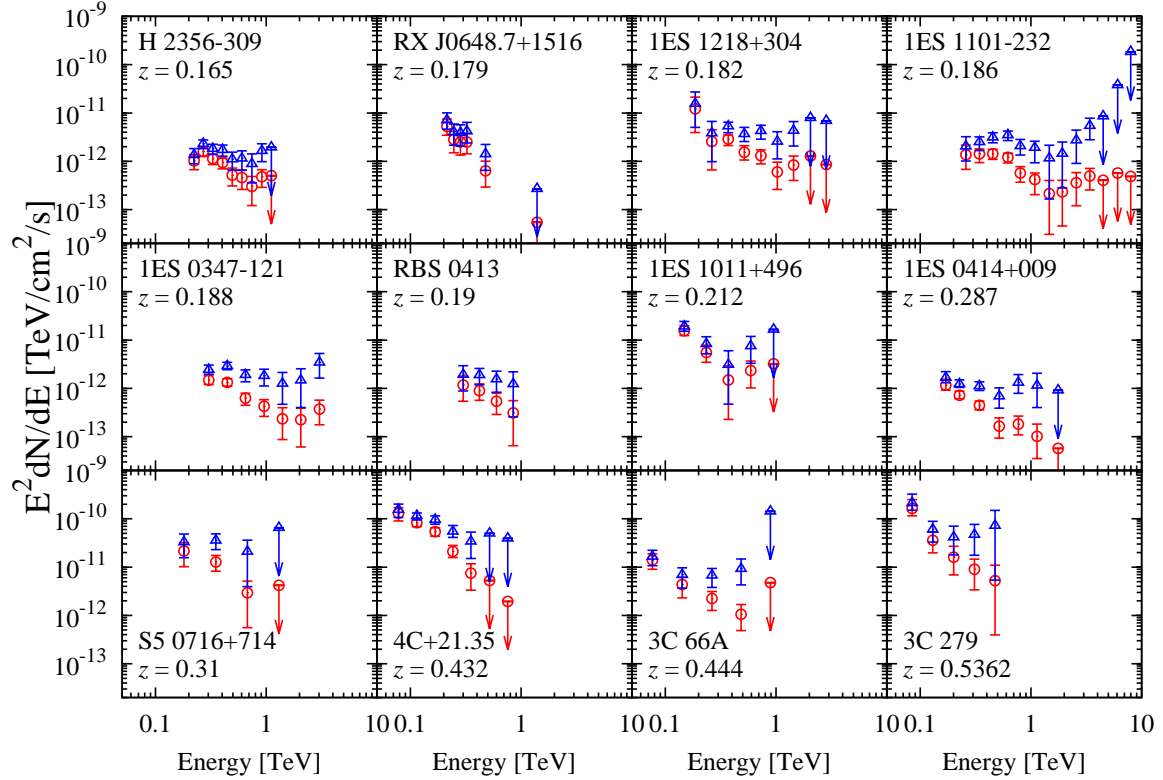


FIG. 14.— Same as Fig. 13, but showing sources at $z > 0.15$. References for data are H 2356-309 (Aharonian et al. 2006b), RX J0648.7+1516 (Aliu et al. 2011), 1ES 1218+304 (Acciari et al. 2009b), 1ES 1101-232 (Aharonian et al. 2007a), 1ES 0347-121 (Aharonian et al. 2007b), RBS 0413 (Aliu et al. 2012), 1ES 1011+496 (Albert et al. 2007b), 1ES 0414+009 (Abramowski et al. 2012a), S5 0716+714 (Anderhub et al. 2009), 4C+21.35 (Aleksić et al. 2011a), 3C 66A (Aleksić et al. 2011b), 3C 279 (Albert et al. 2008).

- Acciari, V. et al. 2009a, *ApJ*, 690, L126
 Acciari, V. A. et al. 2008, *ApJ*, 684, L73
 —. 2009b, *ApJ*, 695, L370
 —. 2010, *ApJ*, 715, L49
 Ackermann, M. et al. 2011, *TeV Particle Astrophysics 2011*
 Actis, M. et al. 2011, *Experimental Astronomy*, 32, 193
 Aharonian, F., Essey, W., Kusenken, A., & Prosekin, A. 2012, *arXiv:1206.6715*
 Aharonian, F. et al. 2002, *A&A*, 384, L23
 —. 2005a, *A&A*, 436, L17
 —. 2005b, *A&A*, 442, 895
 —. 2006a, *Nature*, 440, 1018
 —. 2006b, *A&A*, 455, 461
 —. 2007a, *A&A*, 470, 475
 —. 2007b, *A&A*, 473, L25
 —. 2007c, *A&A*, 475, L9
 Albert, J. et al. 2007a, *ApJ*, 666, L17
 —. 2007b, *ApJ*, 667, L21
 —. 2007c, *ApJ*, 663, 125
 —. 2007d, *ApJ*, 669, 862
 —. 2008, *Science*, 320, 1752
 Aleksić, J. et al. 2011a, *ApJ*, 730, L8
 —. 2011b, *ApJ*, 726, 58
 —. 2012, *A&A*, 539, A118
 Aliu, E. et al. 2011, *ApJ*, 742, 127
 —. 2012, *ApJ*, 750, 94
 Anderhub, H. et al. 2009, *ApJ*, 704, L129
 Anders, E., & Grevesse, N. 1989, *Geochim. Cosmochim. Acta*, 53, 197
 Asplund, M., Grevesse, N., Sauval, A. J., & Scott, P. 2009, *ARA&A*, 47, 481
 Atwood, W. B. et al. 2009, *ApJ*, 697, 1071
 Aykatalp, A., & Spaans, M. 2011, *ApJ*, 737, 63
 Barkana, R. & Loeb, A. 2001, *Phys. Rep.*, 349, 125
 Baugh, C. M., Lacey, C. G., Frenk, C. S., Granato, G. L., Silva, L., Bressan, A., Benson, A. J., & Cole, S. 2005, *MNRAS*, 356, 1191
 Bernstein, R. A. 2007, *ApJ*, 666, 663
 Berta, S. et al. 2011, *A&A*, 532, A49
 Bolton, J. S. & Haehnelt, M. G. 2007, *MNRAS*, 382, 325
 Bouwens, R. J., Illingworth, G. D., Franx, M., & Ford, H. 2007, *ApJ*, 670, 928
 —. 2008, *ApJ*, 686, 230
 Bouwens, R. J. et al. 2011a, *Nature*, 469, 504
 —. 2011b, *ApJ*, 737, 90
 —. 2012, *ApJ*, 752, L5
 Bromm, V., & Loeb, A. 2003, *Nature*, 425, 812
 —. 2006, *ApJ*, 642, 382
 Brown, T. M., Kimble, R. A., Ferguson, H. C., Gardner, J. P., Collins, N. R., & Hill, R. S. 2000, *AJ*, 120, 1153
 Bruzual, G. & Charlot, S. 2003, *MNRAS*, 344, 1000
 Bunker, A. J. et al. 2010, *MNRAS*, 409, 855
 Calzetti, D., Armus, L., Bohlin, R. C., Kinney, A. L., Koornneef, J., & Storchi-Bergmann, T. 2000, *ApJ*, 533, 682
 Cambrésy, L., Reach, W. T., Beichman, C. A., & Jarrett, T. H. 2001, *ApJ*, 555, 563
 Cen, R. 2003, *ApJ*, 591, L5
 Chary, R.-R. 2008, *ApJ*, 680, 32
 Choi, J.-H. & Nagamine, K. 2012, *MNRAS*, 419, 1280
 Choudhury, T. R. & Ferrara, A. 2006, *MNRAS*, 371, L55
 Cole, S., Aragon-Salamanca, A., Frenk, C. S., Navarro, J. F., & Zepf, S. E. 1994, *MNRAS*, 271, 781
 Cucciati, O. et al. 2012, *A&A*, 539, A31
 Dahlen, T., Mobasher, B., Dickinson, M., Ferguson, H. C., Giavalisco, M., Kretchmer, C., & Ravindranath, S. 2007, *ApJ*, 654, 172
 Dale, D. A. & Helou, G. 2002, *ApJ*, 576, 159
 Dole, H. et al. 2006, *A&A*, 451, 417
 Domínguez, A. et al. 2011, *MNRAS*, 410, 2556
 Dwek, E. & Arendt, R. G. 1998, *ApJ*, 508, L9
 Dwek, E. & Krennrich, F. 2012, *arXiv:1209.4661*
 Edelman, J., Bowyer, S., & Lampton, M. 2000, *ApJ*, 539, 187
 Elbaz, D., Cesarsky, C. J., Chanial, P., Aussel, H., Franceschini, A., Fadda, D., & Chary, R. R. 2002, *A&A*, 384, 848
 Essey, W., Kalashev, O., Kusenken, A., & Beacom, J. F. 2011, *ApJ*, 731, 51
 Essey, W. & Kusenken, A. 2012, *ApJ*, 751, L11
 Fan, X. et al. 2006, *AJ*, 132, 117
 Fan, Y. Z., Dai, Z. G., & Wei, D. M. 2004, *A&A*, 415, 483
 Fazio, G. G. & Stecker, F. W. 1970, *Nature*, 226, 135
 Fazio, G. G. et al. 2004, *ApJS*, 154, 39
 Fernandez, E. R., Iliev, I. T., Komatsu, E., & Shapiro, P. R. 2012, *ApJ*, 750, 20
 Finkbeiner, D. P., Davis, M., & Schlegel, D. J. 2000, *ApJ*, 544, 81
 Finke, J. D. & Razzaque, S. 2009, *ApJ*, 698, 1761

- Finke, J. D., Razzaque, S., & Dermer, C. D. 2010, *ApJ*, 712, 238
- Franceschini, A., Rodighiero, G., & Vaccari, M. 2008, *A&A*, 487, 837
- Frayer, D. T. et al. 2006, *ApJ*, 647, L9
- Gardner, J. P., Brown, T. M., & Ferguson, H. C. 2000, *ApJ*, 542, L79
- Gilmore, R. C. 2012, *MNRAS*, 420, 800
- Gilmore, R. C., Madau, P., Primack, J. R., Somerville, R. S., & Haardt, F. 2009, *MNRAS*, 399, 1694
- Gilmore, R. C., Somerville, R. S., Primack, J. R., & Domínguez, A. 2012, *MNRAS*, 422, 3189
- Gorjian, V., Wright, E. L., & Chary, R. R. 2000, *ApJ*, 536, 550
- Greiner, J. et al. 2009, *ApJ*, 693, 1610
- Grevesse, N., & Sauval, A. J. 1998, *Space Sci. Rev.*, 85, 161
- Gunn, J. E. & Peterson, B. A. 1965, *ApJ*, 142, 1633
- Hauser, M. G. & Dwek, E. 2001, *ARA&A*, 39, 249
- Hauser, M. G. et al. 1998, *ApJ*, 508, 25
- Heitler, W. 1954, *Quantum theory of radiation* (Clarendon)
- Helgason, K. & Kashlinsky, A. 2012, *ApJ*, 758, L13
- Hopkins, A. M. 2004, *ApJ*, 615, 209
- Hopkins, A. M. & Beacom, J. F. 2006, *ApJ*, 651, 142
- Horiuchi, S., Beacom, J. F., & Dwek, E. 2009, *Phys. Rev. D*, 79, 083013
- Horiuchi, S., Beacom, J. F., Kochanek, C. S., Prieto, J. L., Stanek, K. Z., & Thompson, T. A. 2011, *ApJ*, 738, 154
- Hosokawa, T., Omukai, K., Yoshida, N., & Yorke, H. W. 2011, *Science*, 334, 1250
- Inoue, S., Salvaterra, R., Choudhury, T. R., Ferrara, A., Ciardi, B., & Schneider, R. 2010a, *MNRAS*, 404, 1938
- Inoue, S. et al. 2012, *Astropart. Phys.* submitted
- Inoue, Y. 2011a, *ApJ*, 733, 66
- . 2011b, *ApJ*, 728, 11
- Inoue, Y. for the CTA Consortium. 2011, in *AGN Physics in the CTA Era* (AGN 2011), arXiv:1112.5813
- Inoue, Y., Inoue, S., Kobayashi, M. A. R., Totani, T., Kataoka, J., & Sato, R. 2011, *MNRAS*, 411, 464
- Inoue, Y. & Ioka, K. 2012, *Phys. Rev. D*, 86, 023003
- Inoue, Y., Totani, T., & Mori, M. 2010b, *PASJ*, 62, 1005
- Iwata, I. et al. 2009, *ApJ*, 692, 1287
- Karim, A. et al. 2011, *ApJ*, 730, 61
- Kauffmann, G., White, S. D. M., & Guiderdoni, B. 1993, *MNRAS*, 264, 201
- Kawai, N. et al. 2006, *Nature*, 440, 184
- Keenan, R. C., Barger, A. J., Cowie, L. L., & Wang, W.-H. 2010, *ApJ*, 723, 40
- Kistler, M. D., Yüksel, H., Beacom, J. F., Hopkins, A. M., & Wyithe, J. S. B. 2009, *ApJ*, 705, L104
- Kneiske, T. M., Bretz, T., Mannheim, K., & Hartmann, D. H. 2004, *A&A*, 413, 807
- Kneiske, T. M. & Dole, H. 2010, *A&A*, 515, A19
- Kobayashi, M. A. R., Inoue, Y., & Inoue, A. K. 2012, arXiv:1208.0489
- Kobayashi, M. A. R., Totani, T., & Nagashima, M. 2007, *ApJ*, 670, 919
- . 2010, *ApJ*, 708, 1119
- Komatsu, E. et al. 2011, *ApJS*, 192, 18
- Labbé, I. et al. 2010, *ApJ*, 716, L103
- Lagache, G., Haffner, L. M., Reynolds, R. J., & Tufte, S. L. 2000, *A&A*, 354, 247
- Levenson, L. R. & Wright, E. L. 2008, *ApJ*, 683, 585
- Levenson, L. R., Wright, E. L., & Johnson, B. D. 2007, *ApJ*, 666, 34
- Mackey, J., Bromm, V., & Hernquist, L. 2003, *ApJ*, 586, 1
- Madau, P., Haardt, F., & Rees, M. J. 1999, *ApJ*, 514, 648
- Madau, P. & Pozzetti, L. 2000, *MNRAS*, 312, L9
- Madau, P. & Silk, J. 2005, *MNRAS*, 359, L37
- Makiya, R. et al. in preparation
- Malkan, M. A. & Stecker, F. W. 1998, *ApJ*, 496, 13
- Malkov, M. A. & O’C Drury, L. 2001, *Reports on Progress in Physics*, 64, 429
- Mannucci, F., Buttery, H., Maiolino, R., Marconi, A., & Pozzetti, L. 2007, *A&A*, 461, 423
- Matsumoto, T. et al. 2005, *ApJ*, 626, 31
- Matsuoka, Y., Ienaka, N., Kawara, K., & Oyabu, S. 2011, *ApJ*, 736, 119
- Matsuura, S. et al. 2011, *ApJ*, 737, 2
- Mazin, D. & Raue, M. 2007, *A&A*, 471, 439
- McKee, C. F. & Tan, J. C. 2008, *ApJ*, 681, 771
- McWilliam, A. 1997, *ARA&A*, 35, 503
- Mesinger, A. & Haiman, Z. 2007, *ApJ*, 660, 923
- Mirabel, I. F., Dijkstra, M., Laurent, P., Loeb, A., & Pritchard, J. R. 2011, *A&A*, 528, A149
- Mortlock, D. J. et al. 2011, *Nature*, 474, 616
- Murase, K., Dermer, C. D., Takami, H., & Migliori, G. 2012, *ApJ*, 749, 63
- Nagashima, M., Gouda, N., & Sugiura, N. 1999, *MNRAS*, 305, 449
- Nagashima, M., Yahagi, H., Enoki, M., Yoshii, Y., & Gouda, N. 2005, *ApJ*, 634, 26
- Nagashima, M. & Yoshii, Y. 2004, *ApJ*, 610, 23
- Neronov, A. & Vovk, I. 2010, *Science*, 328, 73
- Oesch, P. A. et al. 2009, *ApJ*, 690, 1350
- Oh, S. P. 2001, *ApJ*, 553, 25
- Ono, Y., Ouchi, M., Shimasaku, K., Dunlop, J., Farrah, D., McLure, R., & Okamura, S. 2010, *ApJ*, 724, 1524
- Ouchi, M. et al. 2004, *ApJ*, 611, 685
- . 2009, *ApJ*, 706, 1136
- . 2010, *ApJ*, 723, 869
- Papovich, C. et al. 2004, *ApJS*, 154, 70
- Pascale, E. et al. 2009, *ApJ*, 707, 1740
- Pawlik, A. H., Schaye, J., & van Scherpenzeel, E. 2009, *MNRAS*, 394, 1812
- Peacock, J. A. 1999, *Cosmological Physics* (Cambridge University Press)
- Primack, J. R., Bullock, J. S., & Somerville, R. S. 2005, in *American Institute of Physics Conference Series*, Vol. 745, *High Energy Gamma-Ray Astronomy*, ed. F. A. Aharonian, H. J. Völk, & D. Horns, 23–33
- Prochaska, J. X., Naumov, S. O., Carney, B. W., McWilliam, A., & Wolfe, A. M. 2000, *AJ*, 120, 2513
- Raue, M. & Mazin, D. 2008, *International Journal of Modern Physics D*, 17, 1515
- Reddy, N. A., Steidel, C. C., Pettini, M., Adelberger, K. L., Shapley, A. E., Erb, D. K., & Dickinson, M. 2008, *ApJS*, 175, 48
- Ricotti, M. & Ostriker, J. P. 2004, *MNRAS*, 352, 547
- Robertson, B. E. 2010, *ApJ*, 713, 1266
- Robertson, B. E. and Ellis, R. S. and Dunlop, J. S. & McLure, R. J. and Stark, D. P. 2010, *ApJ*, 468, 49
- Rodighiero, G. et al. 2010, *A&A*, 515, A8
- Salpeter, E. E. 1955, *ApJ*, 121, 161
- Schaerer, D. 2003, *A&A*, 397, 527
- Schneider, R., Omukai, K., Inoue, A. K., & Ferrara, A. 2006, *MNRAS*, 369, 1437
- Schiminovich, D. et al. 2005, *ApJ*, 619, L47
- Shapley, A. E., Steidel, C. C., Pettini, M., Adelberger, K. L., & Erb, D. K. 2006, *ApJ*, 651, 688
- Sol, H. et al. 2012, *Astropart. Phys.* submitted
- Somerville, R. S., Gilmore, R. C., Primack, J. R., & Domínguez, A. 2012, *MNRAS*, 423, 1992
- Somerville, R. S. & Primack, J. R. 1999, *MNRAS*, 310, 1087
- Stark, D. P., Bunker, A. J., Ellis, R. S., Eyles, L. P., & Lacy, M. 2007, *ApJ*, 659, 84
- Stecker, F. W., Malkan, M. A., & Scully, S. T. 2006, *ApJ*, 648, 774
- . 2012, arXiv:1205.5168
- Tanvir, N. R. et al. 2009, *Nature*, 461, 1254
- The Fermi-LAT Collaboration. 2012, arXiv:1211.1671
- Totani, T., Kawai, N., Kosugi, G., Aoki, K., Yamada, T., Iye, M., Ohta, K., & Hattori, T. 2006, *PASJ*, 58, 485
- Totani, T. & Takeuchi, T. T. 2002, *ApJ*, 570, 470
- Totani, T., Yoshii, Y., Iwamuro, F., Maihara, T., & Motohara, K. 2001, *ApJ*, 550, L137
- Vaccari, M. et al. 2010, *A&A*, 518, L20
- Verma, A., Lehnert, M. D., Förster Schreiber, N. M., Bremer, M. N., & Douglas, L. 2007, *MNRAS*, 377, 1024
- Wheeler, J. C., Sneden, C., & Truran, J. W., Jr. 1989, *ARA&A*, 27, 279
- Wright, E. L. 2004, *New A Rev.*, 48, 465
- Wright, E. L. & Reese, E. D. 2000, *ApJ*, 545, 43
- Wyder, T. K. et al. 2005, *ApJ*, 619, L15
- Xu, C. K. et al. 2005, *ApJ*, 619, L11
- Yajima, H., Choi, J.-H., & Nagamine, K. 2011, *MNRAS*, 412, 411
- Yajima, H., Umemura, M., Mori, M., & Nakamoto, T. 2009, *MNRAS*, 398, 715
- Yoshida, M. et al. 2006, *ApJ*, 653, 988
- Yoshida, N., Bromm, V., & Hernquist, L. 2004, *ApJ*, 605, 579
- Yoshii, Y. & Peterson, B. A. 1994, *ApJ*, 436, 551
- Younger, J. D. & Hopkins, P. F. 2011, *MNRAS*, 410, 2180
- Yüksel, H., Kistler, M. D., Beacom, J. F., & Hopkins, A. M. 2008, *ApJ*, 683, L5